ELSEVIER

Journal of Alloys and Compounds 311 (2000) 283–287

Journal of ALLOYS AND COMPOUNDS

www.elsevier.com/locate/jallcom

Analysis of hydrogen and deuterium absorption kinetics in Pd nanofilms

S.-Y. Liu[a], Y.-H. Kao[b], Y. Oliver Su[b], T.-P. Perng[a,*]

[a]Department of Materials Science and Engineering, National Tsing Hua University, Hsinchu, Taiwan
[b]Department of Chemistry, National Taiwan University, Taipei, Taiwan

Received 20 May 2000; accepted 19 June 2000

Abstract

An electrochemical quartz crystal microbalance was used to study the kinetics of hydrogen or deuterium absorption in a Pd nanofilm. The Pd film in a thickness of 120 nm was deposited on a quartz crystal. Hydrogen was electrolytically charged into the film and monitored by the frequency shift from the microbalance. The kinetics curves of hydrogen or deuterium absorption in the nano-scaled Pd thin film were obtained at reduction potentials ranging from -1.2 to -1.5 V. Based on the Fick's law, the diffusion rates of hydrogen or deuterium in the film were slower than those in bulk Pd by several orders of magnitude. It is proposed that surface effect was the dominant factor for hydrogen/deuterium absorption in the nano-scaled Pd film. By modifying the Fick's law with a first order reaction equation, the kinetics could be interpreted by a surface-controlled process.

Keywords: Pd; Nanofilm; EQCM; Hydrogen; Diffusion; Deuterium; Surface effect

1. Introduction

Palladium and Pd alloys have been widely used as catalyst [1,2], separator [3,4], or sensor [5,6] for hydrogen since the hydrogenation properties of Pd were disclosed in 1886 by Graham. Among them, many applications are correlated with basic properties such as solubility and diffusivity of hydrogen in Pd films. Unfortunately, most of the database are established for bulk Pd [7–10], not for Pd films. There have been very few reports on the characteristics of hydrogen in Pd thin films [11,12]. It has been noted that the diffusivity of H in Pd thin films is smaller than that in bulk Pd at room temperature. Similar results have also been found for hydrogen gas permeation through Pd membranes in different thicknesses [13,14]. In a permeation process, the gas molecules are first physically adsorbed and chemically absorbed on the surface, and then dissociate into atoms at the high-pressure side. Subsequently, the atoms diffuse through the membrane that obeys Fick's law. Finally, the gas atoms recombine and desorb from the surface at the lower pressure side. The rate-limiting step could be either the surface reaction or bulk diffusion. In general, when the membrane thickness is large enough, the diffusion process would dominate the permeation rate of hydrogen. Surface effects can always be neglected in a bulk diffusion-controlled process [15]. However, when the thickness of membrane or hydrogen pressure is decreased, the permeation rate becomes slower than that extrapolated from the bulk permeation process. The non-linear decay phenomenon of diffusion rate in thin films is considered as being caused by the surface effect.

For hydrogen absorption in a Pd thin film, the surface effect and diffusion behavior are similar to those in hydrogen permeation through a membrane sheet. However, when the film thickness is reduced to the nano-scale, surface process becomes more important, and hydrogenation of the thin film may also change the stress state of the film. Therefore, the surface effect or hydrogen diffusion needs to be modified to explain the hydrogen absorption kinetics in Pd nanofilms. In this study, hydrogen or deuterium absorption kinetics in Pd nanofilms was studied using an electrochemical quartz crystal microbalance (EQCM) [16]. By modifying the Fick's law, a first-order saturation equation was introduced to describe the hydrogen absorption kinetics. The surface effect on hydrogen absorption in the nanofilm is discussed.

2. Experimental

The as-received commercial product, 10 MHz polished AT-cut quartz crystal in a thickness of 166 μm, was used as the substrate. Both sides of the quartz crystal came with

---

*Corresponding author. Fax: +886-3-572-3857.
E-mail address: tpp@mse.nthu.edu.tw (T.-P. Perng).

0925-8388/00/$ – see front matter
PII: S0925-8388(00)01128-2

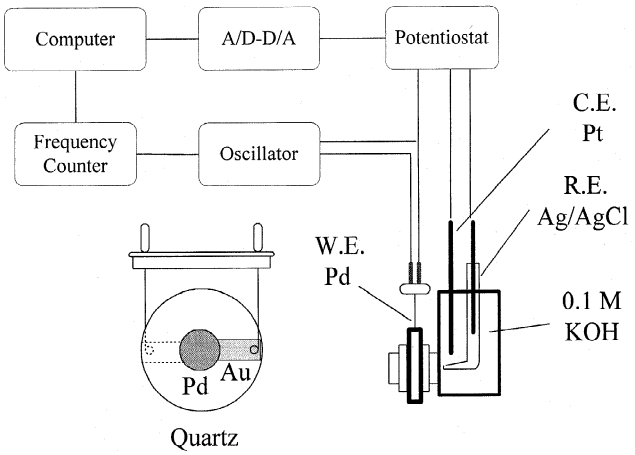

Fig. 1. Schematic diagram of the EQCM and the quartz crystal electrode.

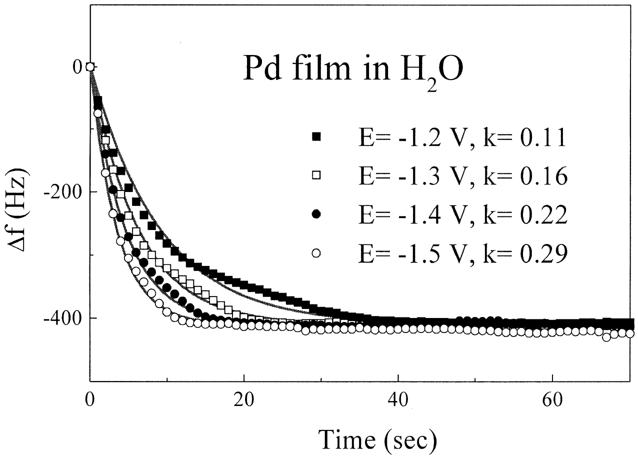

Fig. 2. Hydrogen absorption kinetics curves in the Pd nanofilm at various potentials. The data points are also fitted with different surface constants.

a coating of gold at the center in a thickness of 100 nm and a diameter of 0.5 cm. Each was linked with a 2-mm wide gold line connected to the oscillation circuits. A Pd layer was then deposited on one side of the gold by magnetron sputtering. The thickness of the Pd film identified by a profilometer was approximately 120 nm.

A schematic diagram for the EQCM set-up is shown in Fig. 1. The EQCM system consisted of a 5-ml three-compartment glass cell and resonant oscillation circuits. A 0.1-M KOH solution prepared with light or heavy water was used as the electrolyte. The counter and reference electrodes were Pt and Ag/AgCl, respectively, and the Pd film coated on the quartz crystal was used as the working electrode. The opposite side of the quartz crystal without the Pd coating was exposed to air. The electrolyte was de-aerated by bubbling of nitrogen gas to eliminate oxygen prior to and during the test.

In order to know the reduction potential range for hydrogen and to estimate the amount of hydrogen or deuterium absorbed in the Pd film, the cyclic voltammetry was set to scan from 0 V to −1.5 V, and then back to 0 V at a rate of 5 mV/s. The signals of frequency and current from the electrodes were transferred to a personal computer through an A/D–D/A interface card.

3. Results and discussion

The loops of electrochemical current and frequency shift obtained by cyclic voltammetry and the information that can be derived from the loops have been presented previously [16]. Briefly, the occurrence of hydrogen absorption–desorption in the Pd film could be observed from these curves. Based on the integrated oxidation current and charge conservation law, the amount of hydrogen stored in the film was 181 ng, equivalent to a concentration of H/Pd=0.67. According to Sauerbrey's equation [17], the frequency shift resulted from the mass effect was −210 Hz. Because the total frequency shift, −423 Hz, was caused by the synergistic effects of mass change and the stress induced by hydrogen absorption [16], the frequency shift resulted from the stress effect was −213 Hz. A compressive stress was then calculated to be −1071 MPa based on EerNisse's equation [18], close to the value reported by Cheek and O'Grady [19].

The kinetics curves of frequency shift induced by hydrogen and deuterium absorption at various potentials are shown in Figs. 2 and 3, respectively. The potentials were all located in the hydrogen reduction region to ensure that hydrogen could be charged into the Pd film. The more negative was the applied potential, the more rapid was the absorption rate of hydrogen or deuterium in the Pd thin film. The equilibrium values for all kinetics curves at different potentials were about the same.

A typical electrochemical reaction for hydrogen dissolved in Pd is described as:

$$xH^+ + xe^- + Pd \rightarrow Pd\,H_x \qquad (1)$$

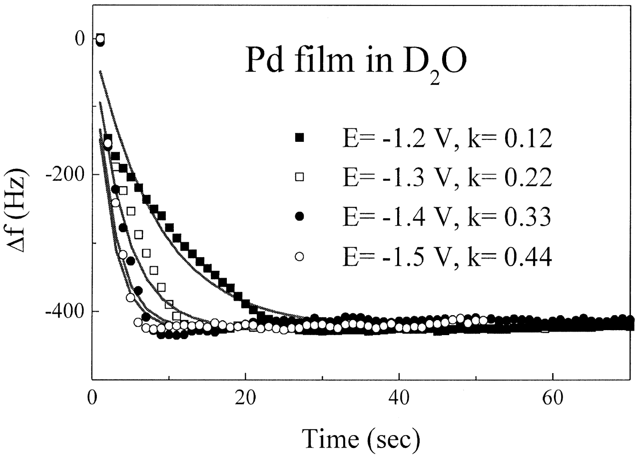

Fig. 3. Deuterium absorption kinetics curves in the Pd nanofilm at various potentials. The data points are also fitted with different surface constants.

where the saturation value for x is about 0.7 at room temperature [20]. The evolution reaction for hydrogen gas molecules on the Pd surface is:

$$2H^+ + 2e^- \rightarrow H_2 \tag{2}$$

Before saturation, most hydrogen atoms are absorbed in the Pd film and few of them are recombined. According to the Nernst equation, the fugacity $f_{H_2}$of hydrogen is an exponential function of overpotential η. Under the equilibrium condition,

$$f_{H_2} = \exp(-2\eta F/RT) \tag{3}$$

where R and T are gas constant and temperature, respectively, and F is the Faraday's constant.

Bockris and Subramanyan have reported that the fugacity in internal cavities is dependent on the mechanism of hydrogen evolution and can be raised by several orders of magnitude in the high-pressure region [21]. From Figs. 2 and 3, the hydrogen absorption rate in the Pd film is increased when the potential is increased. Since hydrogen fugacity is exponentially proportional to the applied negative potential, hydrogen absorption rate is higher at higher fugacities. The change of hydrogen absorption rate slowed down as the potential was high enough.

In general, Fick's second law is used to describe the kinetics of hydrogen or deuterium absorption:

$$\frac{\partial C}{\partial t} = D_H \frac{\partial^2 C}{\partial x^2} \tag{4}$$

The initial and boundary conditions in the Pd film coated on a substrate are given as:

$$C(x, t) = C_0 \quad x = l, t \geq 0 \tag{5}$$

$$\frac{\partial C(x, t)}{\partial x} = 0 \quad x = 0, t \geq 0 \tag{6}$$

where $C(x, t)$ is the hydrogen concentration at time t ($t \geq 0$) and a distance x ($0 \leq x \leq l$) from the interface between the film and the substrate, l is the film thickness; D_H is the diffusivity of hydrogen in Pd, and C_0 is the hydrogen concentration on the Pd surface. The solution of the diffusion equation in a plane sheet can be obtained as: [22]

$$C(x, t) = C_0 \left[1 - \frac{4}{\pi} \sum_0^\infty \frac{(-1)^n}{2n+1} \left(\cos\frac{(2n+1)\pi}{2l} x \right) \times \left(\exp\frac{-D_H(2n+1)^2\pi^2}{4l^2} t \right) \right] \tag{7}$$

From the EQCM measurement, it is noted that each data point of the frequency shift can be used to calculate the average hydrogen concentration in the film. From Eq. (7), by integration to the whole thickness, the average concentration across the thickness is given as:

$$C(t) = C_0 \left[1 - \frac{8}{\pi^2} \sum_0^\infty \frac{1}{(2n+1)^2} \left(\exp\frac{-D_H(2n+1)^2\pi^2}{4l^2} t \right) \right] \tag{8}$$

With hydrogen diffusivity in bulk Pd being typically in the order of ~10^{-7} cm^2/s at room temperature [8], the diffusivities of hydrogen deduced from the curves in Figs. 2 and 3 are all lower by four orders of magnitude. A diffusion barrier on the surface of the film might be the cause for the low effective diffusivities.

To study the surface effect, several theories and experiments have been proposed to interpret the interaction of hydrogen with the surface layer in perfect single crystals and the reconstruction of free surface owing to hydrogen adsorption [23,24]. However, variation of other parameters including the geometric roughness, poisoning by other gases, dissociation rate of hydrogen gas, formation of an electrical double layer in the electrolyte, and the charging pressure or voltage in the gas or electrolyte, respectively, etc., may increase the difficulty to identify the surface properties. The surface effect of a Pd film in the electrolyte involves at least surface reconstruction [23,24] and formation of an electrical double layer in front of the Pd surface [25]. Due to the surface reconstruction, hydrogen can be absorbed into the subsurface. Addition of hydrogen to the sub-surface will result in further reconstruction of the surface structure, and the corresponding energy barrier will be increased as well. The formation of an electrical double layer, mainly caused by adhesion of solvent molecules, specifically adsorbed anions, and solvated cations, obstructs the hydrogen flowing to the surface.

Figs. 4 and 5 show the schematic illustrations for different saturation processes of hydrogen occlusion in thick and nano-scaled Pd films, respectively. For a thick film, a concentration gradient is built through the thickness based on Fick's second law to drive hydrogen diffusion until saturation is reached. The initial surface concentration is dependent on the applied voltage. To reach equilibrium, it takes a much longer time for diffusion in the bulk and to

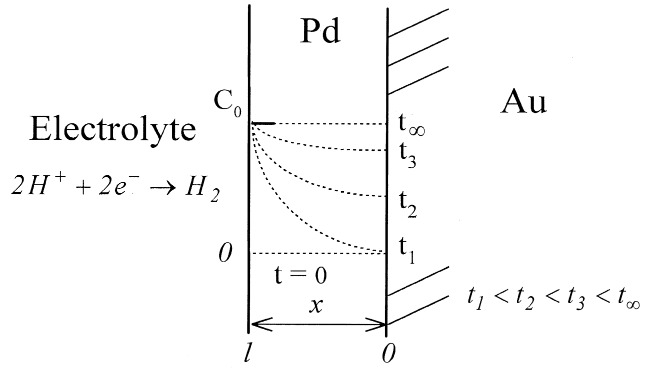

Fig. 4. Hydrogen concentration profiles during absorption in a Pd thick film. C_0 is the initial surface concentration.

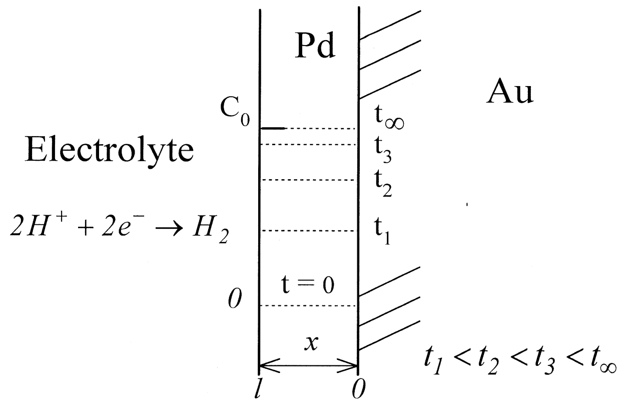

Fig. 5. Hydrogen concentration profiles during absorption in a Pd nanofilm. C_0 is the initial surface concentration.

finish the occlusion so that the surface effect can be ignored. For a nanofilm, however, the thickness of the film is small enough, either the surface barrier or repulsion from the occluded hydrogen in the sublayer could be the rate-limiting step of hydrogen absorption into the nanofilm. Therefore, the diffusion time within the film can be neglected, thus, the concentration profile is treated as a constant value, as shown in Fig. 5. The repulsion from the occluded hydrogen in the sublayer involves the stress induced by lattice expansion, release of reaction heat, and repulsive force between hydrogen atoms.

The influence of surface barrier and repulsion from the occluded hydrogen is not included in Eqs. (7) and (8). If both of them are considered, the average concentration in the film can be assumed to increase exponentially until the saturation is reached, which is described as:

$$\frac{\mathrm{d}C(t)}{\mathrm{d}t} = k(C_0 - C(t)) \tag{9}$$

or

$$C(t) + C_0(1 - \mathrm{e}^{-kt}) \tag{10}$$

where k (unit: s^{-1}) stands for the surface reaction constant and C_0 is the surface concentration (which is also the saturation concentration in the Pd film).

If the surface reaction is the rate-determining step for hydrogen absorption, the diffusion term in the nanofilm can be neglected, the kinetics curves can be fitted with Eq. (10) by adjusting the values of surface reaction constant. For example, in Fig. 2, neglecting the stress effect and if the saturation concentration is substituted with the terminal frequency shift −415 Hz for −1.3 V, k is calculated to be 0.16. The fitted curves for hydrogen and deuterium absorption along with the calculated surface reaction constants are also shown in Figs. 2 and 3, respectively. It is noted that k increases with the applied potential. In effect, k is affected by not only the applied potential but also other factors such as electrolyte, composition, ambient temperature, or applied stress. The surface roughness, grain orientation, film geometry, and grain size, etc., will also influence the absorption rate. In this study, the surface reaction constant in light water was similar to that for heavy water at −1.2 V. At higher applied potentials, the increase in k in heavy water became faster in light water. It implies that the absorption rate of deuterium in Pd nanofilm was faster than that of hydrogen.

In classical theory, the diffusivity ratio of hydrogen to deuterium in most metals is $\sqrt{2}$. It has been frequently observed, however, that reversed isotope dependence is associated with Pd over a broad temperature range from −60 to 200°C [8,26,27]. This inversion has been attributed to a larger activation energy for hydrogen diffusion [8,28]. In the present study, the surface reaction for deuterium also appeared to be faster than for hydrogen. The reason for the absorption rates or higher surface constants for deuterium requires further study.

4. Conclusion

The kinetics of hydrogen/deuterium absorption in a nano-scaled Pd film has been studied by means of EQCM. The surface effect was considered to be the dominant factor in delaying the hydrogen/deuterium absorption rate in the Pd nanofilm. The absorption kinetics models for thick and nanoscaled Pd films are proposed to interpret the hydrogen/deuterium absorption behavior without and with the surface effect, respectively. A first-order reaction is proposed to interpret the surface-controlled absorption in the nanoscaled Pd film. The surface reaction constants are obtained for different applied voltages and electrolytes. The absorption rates as well as the surface reaction constants of deuterium were larger than those of hydrogen.

Acknowledgements

This work was supported by the National Science Council of ROC under Contract Nos. NSC 88-2216-E-007-048 and NSC 87-TPC-M-002-001.

References

[1] V.M. Gryaznov, Platinum Met. Rev. 36 (1992) 70.
[2] M.J. Cole, Platinum Met. Rev. 12 (1981) 25.
[3] F.A. Lewis, X.Q. Tong, R.V. Bucur, Platinum Met. Rev. 35 (1991) 138.
[4] Y.K. Cho, K. Han, K.H. Lee, J. Membrane Sci. 140 (1995) 219.
[5] V.I. Anisimkin, I.M. Kotelyanskii, P. Verardi, E. Verona, Sensors and Actuators B 23 (1995) 203.
[6] R.C. Thomas, R.C. Hughes, J. Electrochem. Soc. 144 (1997) 3245.
[7] F.A. Lewis, The Palladium Hydrogen System, Academic Press, New York, 1967.
[8] J. Völkl, G. Wollenweber, K.H. Klatt, G. Alefeld, Z. Naturforsch 26 (1971) 922.

[9] E. Wicke, H. Brodowsky, in: G. Alefeld, J. Völkl (Eds.), Hydrogen in Metals II, Springer-Verlag, Berlin, 1978.

[10] R.V. Bucur, E. Indrea, Acta Metall. 35 (1987) 1325.

[11] Y. Li, Y.-T. Chen, Int. J. Hydrogen Energy 21 (1996) 281.

[12] H. Hagi, Mater. Trans. JIM 31 (1990) 954.

[13] E. Serra, M. Kemali, A. Perujo, D.K. Ross, Metall. Trans. A 29A (1998) 1203.

[14] A. Khan, K.J. Dietz, F.G. Waelbroeck, P. Wienhold, J. Nucl. Mater. 77 (1978) 337.

[15] C.-L. Yu, T.-P. Perng, Acta Metall. 39 (1991) 1091.

[16] S.-Y. Liu, Y.-H. Kao, Y. Oliver Su, T.-P. Perng, J. Alloy Comp. 293–295 (1999) 468.

[17] G. Sauerbrey, Z. Phys. 155 (1959) 206.

[18] E.P. EerNisse, J. Appl. Phys. 43 (1972) 1330.

[19] G.T. Cheek, W.E. O'Grady, J. Electroanal. Chem. 277 (1990) 341.

[20] Y. Fukai, The Metal-Hydrogen System, Springer, New York, 1993.

[21] J.O'M. Bockris, P.K. Subramanyan, Electrochim. Acta 16 (1971) 2169.

[22] J. Crank, The Mathematics of Diffusion, Oxford University Press, London, 1975.

[23] B.-S. Kang, K.-S. Sohn, Phys. B 205 (1995) 163.

[24] B.-S. Kang, K.-S. Sohn, Phys. B 217 (1996) 160.

[25] A.J. Bard, L.R. Faulkner, Electrochemical Methods, John Wiley and Sons, Singapore, 1980.

[26] C.-T. Lihn, C.-C. Wan, T.-P. Perng, J Appl. Electrochem. 25 (1995) 61.

[27] G. Bohmholdt, E. Wicke, Z. Physik. Chem. N.F. 56 (1967) 133.

[28] S. Majorowski, B. Baranowski, J. Phys. Chem. Solids 43 (1982) 1119.